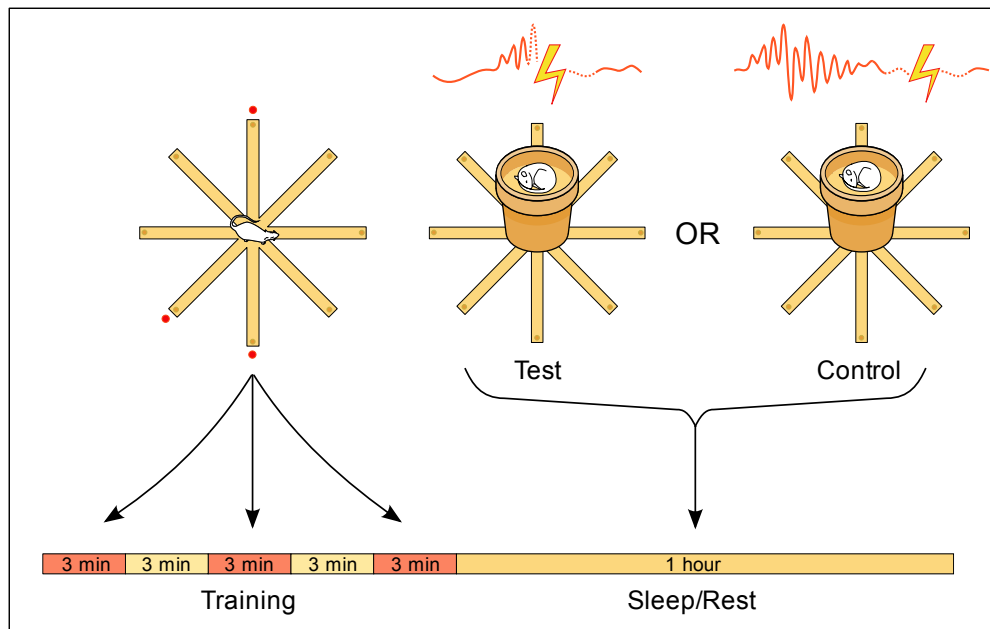
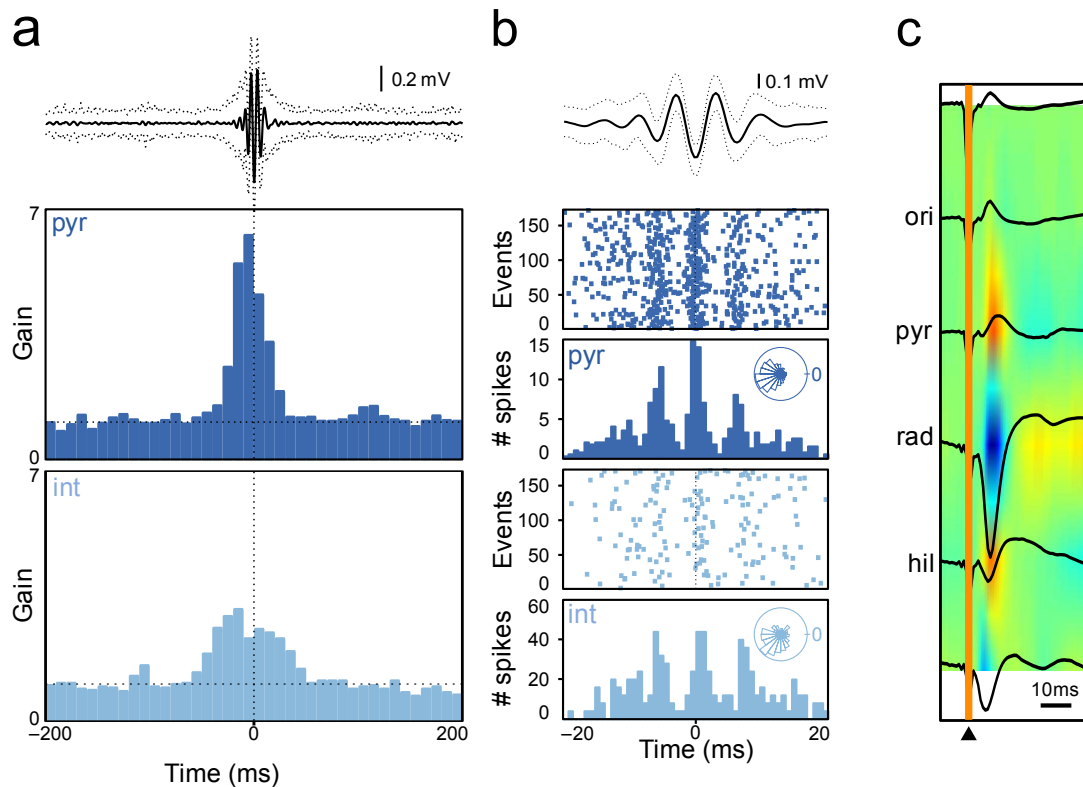


# Selective suppression of hippocampal ripples impairs spatial memory

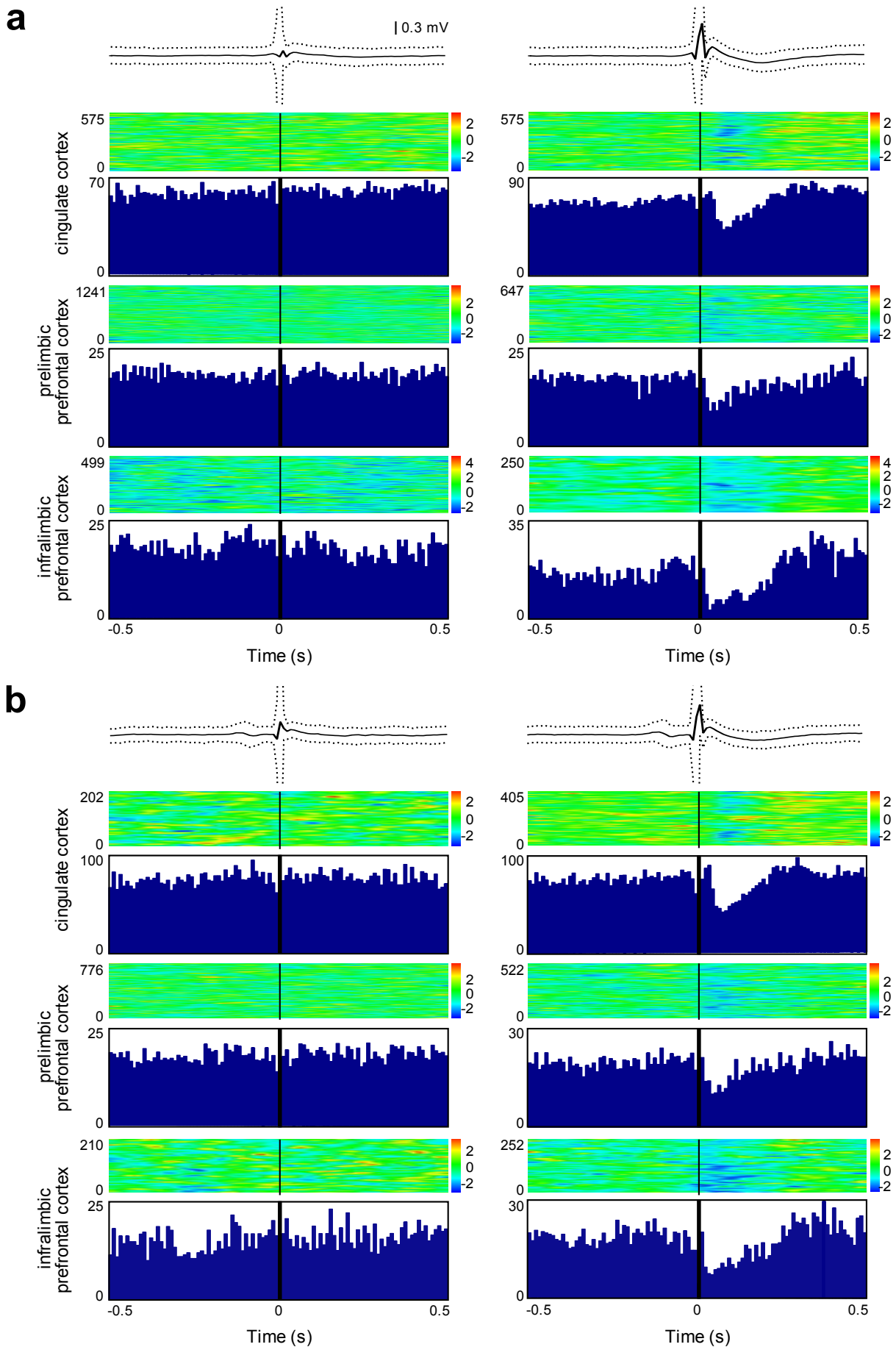
Gabrielle Girardeau, Karim Benchenane, Sidney I. Wiener, György Buzsáki, Michaël B. Zugaro



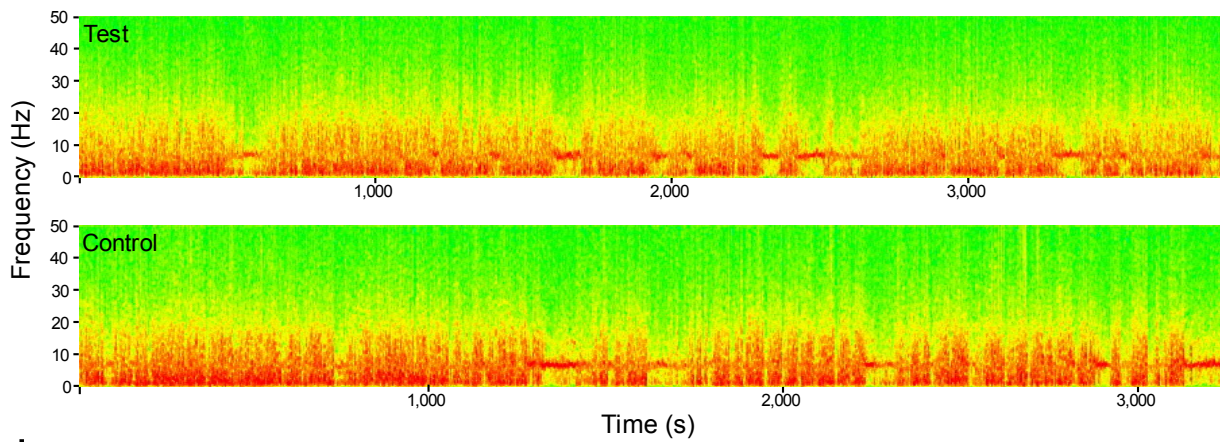
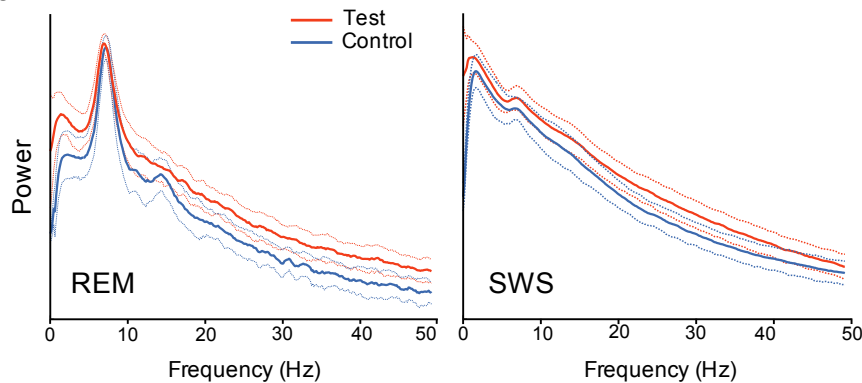
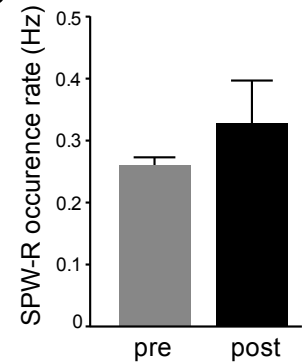
**Supplementary Figure 1.** Training and recording protocol. The rats were allowed to perform three trials each day with the same three arms baited once per trial with chocolate cereal (left, red dots). After the third trial the rat was allowed to rest/sleep in the flowerpot for one hour during which stimulations were triggered, either during (test rats, middle) or outside SPW-R (stimulation control rats, right).



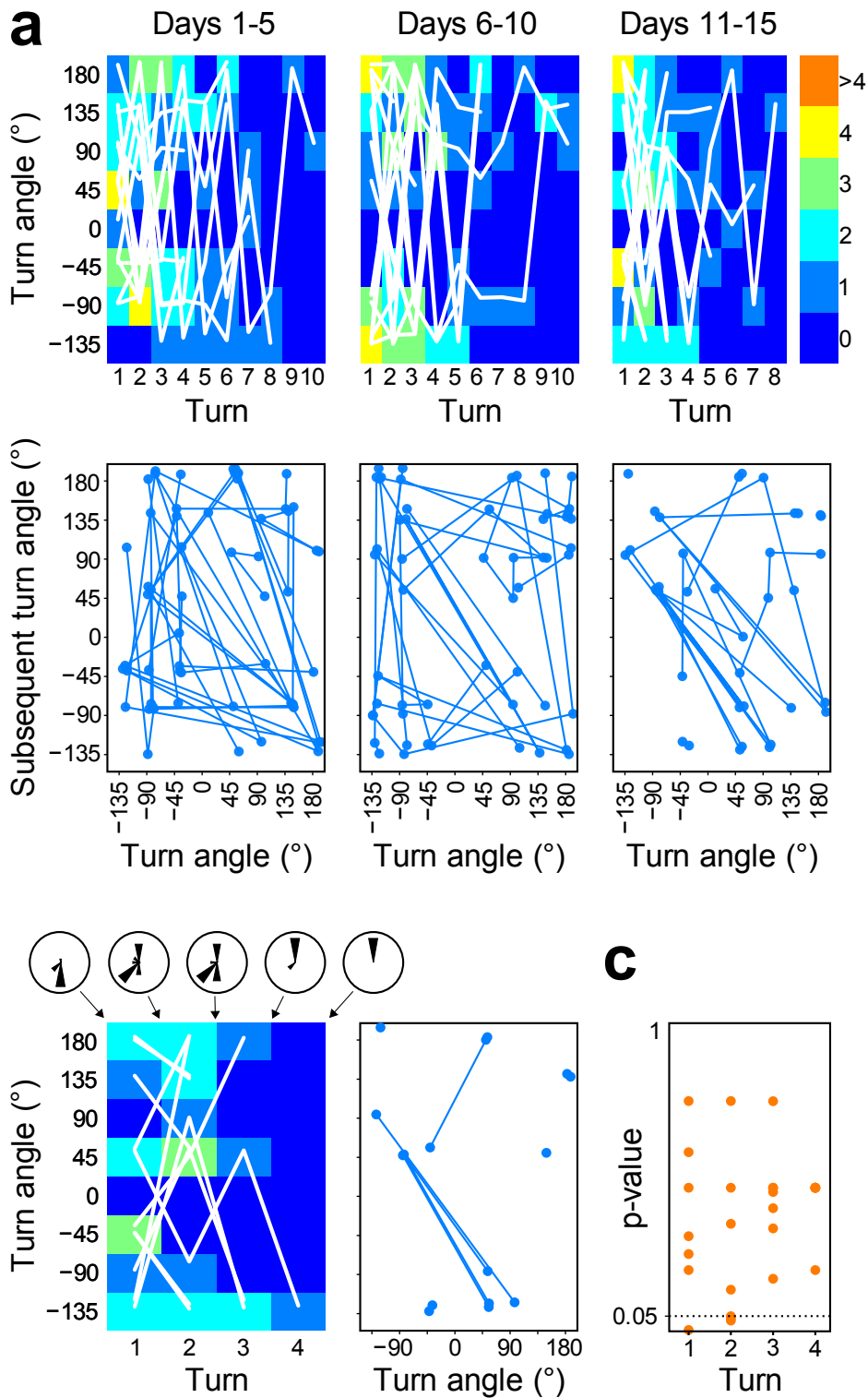
**Supplementary Figure 2.** Ripples and commissural stimulation properties. **(a)** Hippocampal cell discharge increases several-fold during ripples. Average ripple trace (upper panel, dotted lines: 95% confidence intervals) and associated gain in firing rate of pyramidal cells (dark blue) and interneurons (light blue). **(b)** Phase-locked discharge of hippocampal pyramidal cells (dark blue) and interneurons (light blue) during ripple oscillation. Insets: polar plots of spike phase distribution. **(c)** Average current source density of evoked responses (black traces) at multiple depths (n=500). Note the large sink in stratum radiatum (rad, blue) and source in the pyramidal layer (pyr, red). Scale bar: 10 ms, hil: hilus, ori: stratum oriens.



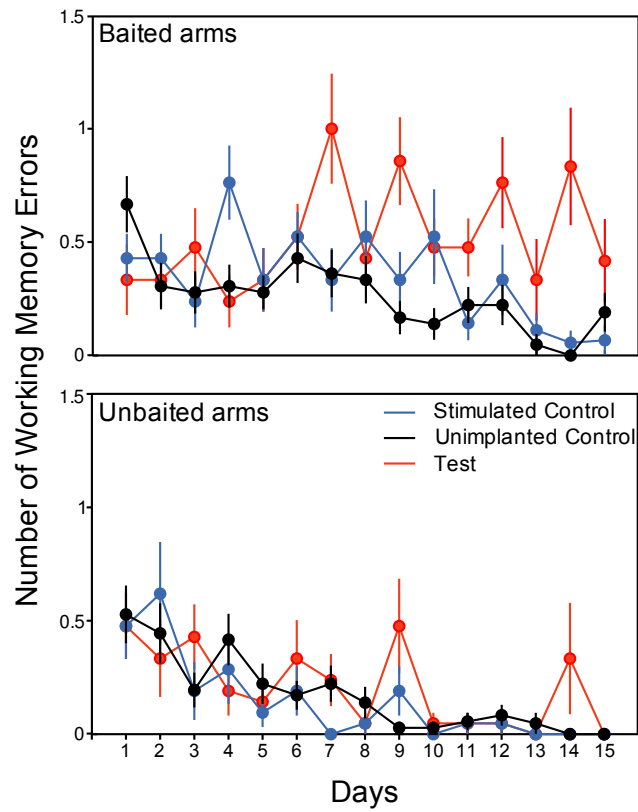
**Supplementary Figure 3.** At the stimulation magnitude used for the experiment, stimulation does not affect the global firing rate of neurons in anterior cingulate cortex and prefrontal cortex (prelimbic and infralimbic). **(a)** Color plots and peri-event time histograms of the multi-unit spiking activity centered on the stimulations, for the test condition (the stimulation interrupts the ripple). Left column, weak stimulation (at or below hippocampal population spike threshold; experimental condition). The global firing rate is not affected. Right column, strong stimulations (maximal hippocampal population spike amplitude) induce a delayed decrease of the global population firing rates. Black traces, mean hippocampal local field potentials around stimulation times (dotted lines, 95% confidence intervals). **(b)** Same as in **a** for the control condition (stimulations outside the ripples). Test and control conditions yield similar effects (left columns in **a** and **b**).

**a****b****c**

**Supplementary Figure 4.** Stimulation does not affect global sleep structure. **(a)** Examples of power spectrograms of hippocampal local field potentials recorded during a sleep session in a test and a control rat. **(b)** Average spectra during REM-sleep and SWS (same rats as in **a**, dotted lines: SD). Note the strong power in the theta band (7~12 Hz) during REM-sleep and in the delta band (1~4 Hz) during SWS. **(c)** Mean SPW-R occurrence rates before and after stimulation sessions in test rats are not significantly different (t-test,  $n=7$ , NS), indicating that suppression of ripples for one hour of rest/sleep did not induce a 'rebound' phenomenon during subsequent sleep.



**Supplementary Figure 5.** Test rats do not develop stereotypical turning strategies in the radial maze task. **a.** Simple locomotor strategies were investigated in successive blocks of 5 days of training. Upper panels: the incidence of successive turn angles for a representative rat is represented on a color scale, e.g. the yellow square in the bottom left corner for days 6-10 indicates that in 4 trials, the rat turned by  $-135^\circ$  on the first turn. White lines connect successive turns of the same trial. Lower panels: return map of successive turn angles. Each angle is represented as a function of the previous angle, and successive angles in single trials are connected with blue lines. Stereotyped turning strategies would yield superimposed curves. **b.** Simple locomotor strategies were further investigated for the last 5 days of training, including only trials with a maximum of 2 errors (performance index  $\geq 0.56$ ). Corresponding arm visits are shown as polar histograms. Data are from the same rat as in **(a)**. **c.** Group data for days 10-15, including only trials with a maximum of 2 errors. For each successive turn, we tested whether the distribution of angles was uniform (Rayleigh tests). p-values below 0.05 (dotted line) correspond to single-peaked distributions, i.e. instances where the rat generally turned by the same angle, indicating stereotypy.



**Supplementary Figure 6.** Mean working memory errors (returning to an arm that was already visited during the same trial) in baited (*upper panel*) and unbaited arms (*lower panel*). Note that on average the rats do not make more than one working memory error per trial. *Error bars:* s.e.m.

## Supplementary Methods

**Surgery.** Fourteen male Long Evans rats (René Janvier, Le Genest, St Isle, France) were bilaterally implanted with four independently movable single-wire electrodes (70  $\mu\text{m}$  stainless steel,  $n=11$ ) or two 9-site silicon probes (NeuroProbes<sup>1-3</sup>, 200  $\mu\text{m}$  spacing,  $n=3$ ) in the dorsal hippocampus (ML  $\pm 2.5$ , AP  $-3.5$  relative to bregma). Three additional rats were implanted, two with tetrodes (groups of four twisted 12  $\mu\text{m}$  nichrome wires) in the hippocampus and overlying neocortex, and one with electrodes in hippocampus and anterior cingulate and prefrontal cortices (AP  $+2.7$ , ML  $+0.5$ ), for preliminary experiments (shown in Fig. 2 and Supplementary Fig. 3). Bipolar stimulation electrodes (60  $\mu\text{m}$  stainless steel) were implanted in the ventral hippocampal commissural pathway (ML  $\pm 1.1$ , AP  $-1.3$ , DV  $-3.8$  relative to bregma). During recovery from surgery (minimum 3 days), the rats received food and water *ad libitum*. The recording electrodes were then progressively lowered until they reached the CA1 pyramidal layer, where ripples were recorded. Meanwhile, rats were habituated to the 8-arm radial maze, and maintained on food restriction at 85% of their normal weight. All experiments were in accord with institutional (CNRS Comité Opérationnel pour l'Ethique dans les Sciences de la Vie), international (NIH guidelines) standards and legal regulations (Certificat no. 7186, Ministère de l'Agriculture et de la Pêche) regarding the use and care of animals.

**Training sessions.** The rats were trained to find food rewards on an 8-arm radial maze where three of the arms were baited. Training occurred during the light cycle, either in the morning (9:00) or in the afternoon (14:30) with equal distribution in all groups. The same spatial configuration of rewards was used for all rats in all training sessions (Supplementary Fig. 1). Salient visual cues suspended on the walls of the room served as spatial reference cues. Each session consisted of three trials on the maze, separated by 3 min rest periods when the rat was secluded in a flowerpot in the center of the maze. On each trial, the rat was removed from the maze as soon as it had found the three rewarded arms, or after a maximum of three minutes of exploration. After completion of the three trials, the animals were placed in the flowerpot in the center of the maze for the immobility/sleep stimulation session (1 hour). During training and post-training recording sessions, the experimenter remained outside the maze area enclosed by black curtains, and behavior was monitored using an overhead video camera.

**Recording and stimulation.** Brain signals were preamplified (unity-gain, Noted Bt, Pécs, Hungary), amplified 1000x (Neuralynx L8, Bozeman, MT, USA), acquired and digitized using two synchronized Power1401 systems (CED, Cambridge, UK). Online detection of the ripples (threshold crossing on the bandpass-filtered signal) automatically triggered a single-pulse (0.5 ms) commissural stimulation. This recruited principal cells and interneurons throughout both hippocampi and dentate gyri (via commissural fibers bilaterally connecting CA3-CA3, CA3-DG and DG-DG, and Schaffer collaterals connecting CA3-CA1), inducing transient silencing of the hippocampal network due to a combination of GABA receptor-mediated inhibition,  $\text{Ca}^{2+}$ -dependent  $\text{K}^{+}$  conductance increase and disfacilitation. In test rats the stimulation was triggered by the onset of the ripples (detection-stimulation) whereas in control rats stimulation was delayed by a random interval of 80 to 120 ms (detection-delay-stimulation, Fig. 1), so that the stimulation occurred outside the detected ripple. Hence, our stimulation protocol ensured that any potential performance deficit of the test rats could be specifically attributed to the selective suppression of ripples rather than to other non-specific effects of hippocampal stimulation. Online detection rate for test rats was calculated as  $N/(n+N)$  where  $N$  is the number of on-line ripple-triggered stimulations, and  $n$  is the number of remaining ripples detected offline using the same LFP (see below). In both cases (test and control) the number of stimulations was limited to 5 per second. Because at lower stimulus intensities, silencing of hippocampal activity lasted for less than  $\sim 100$  ms (Fig. 1), in the behavioral

experiments we used low intensities for selective and transient perturbation of the hippocampal network activity. The stimulation voltage was thus adjusted for each animal to the minimum value necessary to interrupt the ripples (5~30 V).

Recordings were visualized and processed using NeuroScope and NDManager<sup>4</sup> (<http://neuroscope.sourceforge.net>, <http://ndmanager.sourceforge.net>). Spike sorting was done using the semi-automatic spike classifier KlustaKwik (<http://klustakwik.sourceforge.net>) and the graphical spike sorting application Klusters<sup>4</sup> (<http://klusters.sourceforge.net>).

**Data analysis.** In accordance with standard procedures to perform ANOVAs on proportion data, behavioral performance was computed as  $p=2/\pi.\arcsin(\sqrt{(n/N)})$ , where  $n$  is the number of baited arms visited by the rat, and  $N$  is the total number of visits. Data were analyzed using custom software developed in Matlab (The Mathworks, Inc., Natick, MA, USA). Spectrograms were constructed using chronux (<http://www.chronux.org>).

Chance performance was computed using a bootstrap procedure. Because chance performance depends on the number of working memory (WM) errors, which is *a priori* unknown, we estimated its lower and upper bounds. These correspond to the following two scenarios. In the first scenario (lower chance level), the rat randomly chooses any one arm on each sequential visit (indefinite number of WM errors). In the second scenario (upper chance level), the rat chooses each sequential arm randomly but never visits the same arm twice (no WM errors). The actual chance performance lays between these two bounds. Analyses used the more conservative upper chance level.

Offline ripple detection was performed by band-pass filtering (100~200 Hz), squaring and normalizing, then thresholding the field potential recorded in CA1 pyramidal layer. Ripples were defined as events peaking at >5 standard deviations and lasting <100 ms. Sleep stages (SWS/REM) were determined by automatic K-means clustering of the theta/delta ratio extracted from the power spectrograms during the episodes where the animal was immobile (linear velocity < 3 cm/s for at least 30 s, with brief movements < 0.5 s).

## Supplementary References

1. Herwik, S., Kisban, S., Aarts, A. A. A., Seidl, K., Girardeau, G., Benchenane, K., Zugaro M. B., Wiener, S. I., Paul, O., Neves, H. P. & Ruther, P. Fabrication technology for silicon-based microprobe arrays used in acute and sub-chronic neural recording. *J. Micromech. Microeng.* **19**, (2009)
2. Neves, H.P., Orban, G.A., Koudelka-Hep, M., Stieglitz, T. & Ruther, P. Development of modular multifunctional probe arrays for cerebral applications. *Neural Engineering*, CNE '07. 3rd International IEEE/EMBS Conference, 104-9 (2007).
3. Ruther, P., Aarts, A.A., Frey, O., Herwik, S., Kisban, S., Seidl, K., Spieth, S., Schumacher, A., Koudelka-Hep, M., Paul, O., Stieglitz, T., Zengerle, R., & Neves, H. The NeuroProbes project - multifunctional probe arrays for neural recording and stimulation. *Biomed. Tech.*, **53** (suppl.1), 238-240 (2008).
4. Hazan, L., Zugaro, M. & Buzsáki, G. Klusters, Neuroscope, NDManager: a free software suite for neurophysiological data processing and visualization. *J. Neurosci. Methods* **155**, 207-216 (2006).